

## Intelligent Delineation Algorithm of Urban Development Boundary Based on Graph Neural Network

Yu Li<sup>\*</sup>, Xinzi Ma

*Department of Art and Design, Beijing City University, Shunyi District, Beijing, China*

**Abstract:** The Urban Growth Boundary (UGB) is essential for controlling urban sprawl and optimizing land use, yet traditional delineation methods struggle with modeling complex spatial relationships and fusing multi-source data. This study proposes an intelligent UGB delineation algorithm based on a Graph Neural Network (GNN). The study area is discretized into uniform spatial units to construct an urban graph, with node features integrating remote sensing imagery, land use types, transportation networks, and population-economic data. A spatially constrained graph convolution structure with an improved attention mechanism is designed to jointly model spatial structures and expansion driving factors, enhanced by multi-scale feature aggregation and spatial consistency constraints. Experimental validation in a 1,250 km<sup>2</sup> urban area (5,024 nodes, approximately  $3.8 \times 10^4$  edges) demonstrates that the proposed model achieves 0.912 accuracy and 0.900 F1-score in UGB recognition—3.4% and 3.8% higher than traditional GCN—with a 7.2% improvement in spatial consistency. The model remains stable across 250–1000 m spatial scales, indicating strong generalization ability and spatial adaptability. This GNN-based UGB delineation method effectively captures urban spatial structure characteristics and expansion patterns, providing a high-precision, data-driven technical pathway for territorial spatial planning and sustainable urban growth management.

**Keywords:** Urban growth boundary; Graph neural network; Urban expansion prediction; Spatial planning; Multi-source data fusion

**How to Cite:** Li, Y., & Ma, X. (2026). Intelligent delineation algorithm of urban development boundary based on graph neural network. *International Scientific Technical and Economic Research*, 4(1), 123–148. <https://doi.org/10.71451/ISTAER2606>

**Article history:** Received: 26 Dec 2025; Revised: 18 Feb 2026; Accepted: 03 Mar 2026; Published: 15 Mar 2026  
**Copyright:** © 2026 The Author(s). Published by Sichuan Knowledgeable Intelligent Sciences. This is an open access article under the [CC BY 4.0 license](http://creativecommons.org/licenses/by/4.0/) (<http://creativecommons.org/licenses/by/4.0/>).

### 1. INTRODUCTION

With the continuous advancement of global urbanization and the acceleration of urban spatial expansion, the contradiction between land resource utilization and ecological environment protection has become increasingly prominent. In this context, the UGB, as an important tool in territorial spatial planning systems, is widely used to control urban sprawl, optimize land use structures, and protect ecological space [1],[2],[3]. UGB guides urban growth toward intensive and sustainable development by delineating the scope of urban construction and development over a certain future period. However, in actual planning practice, the

<sup>\*</sup>**Corresponding author:** Yu Li, Department of Art and Design, Beijing City University, Shunyi District, Beijing, China. Email: [15001136468@163.com](mailto:15001136468@163.com)

delineation of urban development boundaries faces many challenges. On the one hand, urban spatial structure is highly complex. Urban expansion is influenced not only by land use conditions, but also by factors such as traffic accessibility, population distribution, economic development, and the natural environment [4],[5],[6]. On the other hand, urban expansion exhibits clear spatial correlation and dynamic evolution, with significant interactions between different regions. This makes UGB delineation a complex spatial decision-making problem. Therefore, how to achieve a scientific, reasonable and highly automated delineation of urban development boundary based on the comprehensive consideration of a variety of spatial factors has become an important issue in the current territorial spatial planning.

Traditional methods for delineating urban development boundaries mainly rely on planning expert experience, spatial statistical analysis, and rule-driven models. For example, land suitability evaluation, the Analytic Hierarchy Process (AHP), multi-index comprehensive evaluation, and cellular automata (CA) models are used to predict urban expansion trends and delineate development boundaries accordingly [7]. While such methods have played an important role in early urban planning research, they still have notable limitations in dealing with complex spatial relationships. Firstly, traditional methods are often based on linear or semi empirical models, which are difficult to effectively describe the nonlinear relationships in urban spatial systems. Secondly, many methods rely on manual setting of rules or parameters, which results in strong subjectivity and is difficult to adapt to different urban development scenarios [8],[9]. In addition, in the large-scale spatial data environment, the traditional methods also have shortcomings in the automatic analysis ability and calculation efficiency, and it is difficult to make full use of the current remote sensing data, geographic information data, socio-economic data and other multi-source information. Therefore, it is of great significance to explore new methods that can effectively integrate multi-source spatial data and automatically learn complex spatial structure relationships for improving the scientific and intelligent level of UGB delineation.

In recent years, the advancement of deep learning has enabled Graph Neural Networks (GNNs) to show significant advantages in modeling data with complex structures. Unlike traditional neural networks, which mainly deal with regular grid data, graph neural networks can directly deal with graph data with topological structure, and learn complex relational structure through the information transmission mechanism between nodes [10],[11]. In an urban spatial system, there are significant adjacency and spatial dependencies between different spatial units, which can be naturally represented as a graph structure. For example, urban parcels, spatial grids or planning units can be regarded as nodes in the graph, while adjacency or traffic links can be represented as edges. Through graph neural networks, we can achieve joint learning from multi-source data while preserving the spatial topology, thereby more accurately capturing the patterns of urban spatial development. In addition, graph neural network can gradually capture the larger scale spatial dependence through multi-layer information transmission, which makes it have broad application prospects in the fields of urban expansion prediction, land use change analysis and spatial planning decision support. Therefore, applying graph neural networks to delineate urban development boundaries provides a new technical pathway for achieving intelligent UGB recognition.

Against this background, this study proposes an intelligent algorithm for delineating urban development boundaries based on graph neural networks. Firstly, the research area is divided into uniform scale spatial units, and the urban spatial map structure is constructed. The spatial units are represented as nodes, and the spatial adjacency relationship is represented as edges, so as to form the urban spatial map data. On this basis, multi-dimensional node feature representation is constructed by fusing remote sensing images, land use data, traffic network data, population and economic statistics and other multi-source information. Then, a graph neural network model for UGB recognition task is designed, which learns the characteristics of urban spatial structure through the mechanisms of spatial feature coding, graph volume information dissemination and multi-scale feature aggregation, and the spatial constraint mechanism and the embedding of urban expansion driving factors are introduced into the model

to improve the expression ability of the model to the laws of urban development [12],[13]. Finally, the continuous urban development boundary is generated through the node classification results to achieve automatic UGB delineation. The framework can automatically learn the urban expansion mode in the complex spatial data environment, and provide a data-driven intelligent solution for the delineation of urban development boundaries [14].

The main contributions of this study are as follows. Firstly, starting from the structural characteristics of urban spatial system, an urban spatial representation model based on graph structure is constructed, enabling multi-source geospatial data to be fused and analyzed within a unified framework. Secondly, aiming at the task of identifying the boundary of urban development, an improved graph neural network algorithm is proposed. By introducing the spatial constraint mechanism and embedding the driving factors of urban expansion, the expression ability of the model on the relationship between urban development dynamics and spatial structure is effectively improved. Thirdly, by designing adaptive neighborhood weight and improving graph attention mechanism, the model can more accurately identify key spatial units, so as to improve the accuracy of UGB prediction. Finally, the effectiveness and stability of the proposed method in UGB delineation task are verified by system experiments, and the results show that the method is superior to the traditional model in accuracy and spatial consistency. The research results provide a new technical idea for intelligent decision-making in urban spatial planning, and also provide a useful exploration for the application of graph neural network in the field of geospatial analysis.

## 2. URBAN SPATIAL MAP STRUCTURE MODELING AND MULTI-SOURCE DATA EXPRESSION

To effectively describe the complex spatial interactions between urban spatial units, this study abstracts the study area as an attributed graph  $G = (V, E, X)$ , where  $V = \{v_1, v_2, \dots, v_n\}$  represents the set of urban spatial unit nodes,  $E \subseteq V \times V$  represents the set of spatial relationship edges, and  $X \in \mathbb{R}^{n \times d}$  is the node feature matrix ( $n$  = number of spatial units,  $d$  = feature dimension). Each node  $v_i$  corresponds to a fundamental urban spatial unit (such as regular grid, plot, or planning unit), and its attributes are derived from multi-source geographic data [15]. By discretizing the study area into uniform spatial units, the continuous space problem is transformed into a discrete graph structure learning problem, providing structured input for feature propagation and boundary recognition in subsequent graph neural networks.

For node feature representation, it is necessary to comprehensively describe the land use attributes, development intensity and socio-economic characteristics of urban spatial units. For node  $v_i$ , its eigenvector is defined as:

$$x_i = [f_i^{rs}, f_i^{lu}, f_i^{tr}, f_i^{pop}, f_i^{eco}] \quad (1)$$

Where  $f_i^{rs}$  represents the surface features extracted from remote sensing images, such as building density, vegetation index, or impervious surface ratio;  $f_i^{lu}$  represents the coding characteristics of land use types;  $f_i^{tr}$  represents traffic accessibility indicators, such as road density or distance to major traffic nodes;  $f_i^{pop}$  represents the characteristics of population density;  $f_i^{eco}$  is the indicator of economic development intensity. Through the above multi-dimensional feature vectors, the comprehensive attribute representation of urban spatial units can be constructed [16]. To eliminate the influence of different data scales on model training, each type of feature is normalized, and its standardized form is:

$$\tilde{x}_{ij} = \frac{x_{ij} - \mu_j}{\sigma_j} \quad (2)$$

Where  $x_{ij}$  is the original value of node  $i$  on the  $j$ th feature dimension,  $\mu_j$  and  $\sigma_j$

represent the mean and standard deviation of the feature of this dimension in all nodes respectively. The standardization process can improve the training stability of the model under multi-source data input.

Urban spatial system has obvious neighborhood dependence characteristics, so it is necessary to model spatial adjacency relationship through topological structure. In this study, we use the adjacency matrix  $A \in \mathbb{R}^{n \times n}$  to represent the graph structure, where each element  $A_{ij}$  characterizes the correlation strength between the spatial elements  $v_i$  and  $v_j$ . When two spatial units are spatially adjacent or meet a certain distance threshold, a connection relationship is established in the graph [17]. Its basic expression is:

$$A_{ij} = \begin{cases} 1, & d_{ij} \leq \delta \\ 0, & d_{ij} > \delta \end{cases} \quad (3)$$

Where  $d_{ij}$  represents the spatial distance between node  $v_i$  and  $v_j$ , and  $\delta$  is the neighborhood determination threshold. To further reflect the intensity of spatial interaction, this study introduces the weighted adjacency relationship based on distance attenuation, whose weight form is defined as:

$$w_{ij} = \exp\left(-\frac{d_{ij}^2}{2\sigma^2}\right) \quad (4)$$

Where  $\sigma$  is the spatial scale parameter, which is used to control the influence range of the neighborhood. Through this weight mechanism, the distance attenuation effect between urban spatial elements can be more truly reflected, so that the adjacent areas have higher correlation weight in the graph structure.

In terms of multi-source data expression, urban spatial system involves remote sensing images, land use data, transportation network, population and economic statistics and other information sources. In order to realize the unified expression between different data sources, it is necessary to establish the fusion feature matrix. Let the characteristics of different data sources be expressed as  $X^{rs}, X^{lu}, X^{tr}, X^{pop}, X^{eco}$  respectively, then the comprehensive characteristic matrix can be expressed as:

$$X = [X^{rs} \parallel X^{lu} \parallel X^{tr} \parallel X^{pop} \parallel X^{eco}] \quad (5)$$

Where the symbol  $\parallel$  indicates the feature concatenation operation. The feature concatenation method can achieve a unified representation while maintaining the semantic information of the original data, so that the graph neural network can simultaneously use the multi-dimensional information such as natural environment, traffic structure and socio-economic factors in the process of feature propagation. In order to further enhance the synergy between different data sources, feature projection can also be performed through linear mapping, which is expressed as:

$$H^{(0)} = XW_f \quad (6)$$

Where  $W_f$  is a learnable feature mapping matrix, and  $H^{(0)}$  represents the initial node representation after fusion, which will be used as the input of the subsequent graph neural network.

### 3. FRAMEWORK OF GRAPH NEURAL NETWORK MODEL FOR URBAN DEVELOPMENT BOUNDARY IDENTIFICATION

To realize automatic urban development boundary recognition and spatial structure learning, this study constructs a graph neural network architecture for urban spatial graph data. The model takes the urban spatial graph  $G = (V, E, X)$  as input, progressively extracts

structural relationships and developmental characteristics of spatial units through multi-layer graph feature learning, and finally outputs the urban development boundary prediction [18],[19],[20]. The overall model consists of a spatial feature encoding module, a graph convolution information propagation module, a multi-scale spatial feature aggregation module, and a boundary prediction output layer. Let the input node characteristic matrix be  $X \in \mathbb{R}^{n \times d}$ , where  $n$  is the number of urban spatial units and  $d$  is the node characteristic dimension. The model gradually generates a high-dimensional representation  $H^{(l)}$  through multi-layer nonlinear transformation, and finally obtains the boundary prediction result  $Y$ . The overall expression of the model can be shown as:

$$Y = f_{out} \left( f_{agg} \left( f_{gcn} \left( f_{enc}(X, A) \right) \right) \right) \quad (7)$$

Where  $f_{enc}(\cdot)$  represents the spatial feature encoding function,  $f_{gcn}(\cdot)$  represents the graph convolution propagation process,  $f_{agg}(\cdot)$  represents the multi-scale feature aggregation operation,  $f_{out}(\cdot)$  represents the boundary prediction function, and  $A$  is the adjacency matrix of the urban spatial graph. The overall architecture can achieve the deep expression of complex spatial patterns while preserving the spatial topology.

In the stage of spatial feature coding, the original node features need to be embedded and mapped, so that the data from different sources can be expressed in the unified feature space. Therefore, the feature coding function is introduced to project the input feature matrix  $X$  into a higher dimensional representation space, and its calculation form is:

$$H^{(0)} = \sigma(XW_e + b_e) \quad (8)$$

Where  $W_e \in \mathbb{R}^{d \times h}$  is the feature coding weight matrix,  $b_e$  is the offset term,  $h$  is the hidden feature dimension, and  $\sigma(\cdot)$  is the nonlinear activation function (such as the ReLU function). This encoding operation can effectively enhance the representational power across different data modalities, and make the original spatial attributes more discriminative in the subsequent graph structure learning process. The obtained  $H^{(0)}$  will be represented as the initial node of the graph neural network layer.

In the graph structure learning process, information is propagated and updated between nodes through graph convolution operations. In order to characterize the influence of spatial neighborhood on node characteristics, the normalized adjacency matrix  $\tilde{A}$  is introduced to realize neighborhood information aggregation [21],[22],[23]. Let  $\tilde{A} = D^{-\frac{1}{2}}(A + I)D^{-\frac{1}{2}}$ , where  $I$  is the identity matrix used to add the self connection relationship,  $D$  is the degree matrix, and its diagonal elements are defined as  $D_{ii} = \sum_j (A_{ij} + I_{ij})$ . In the convolution of the  $l$ st layer graph, the node feature update process can be expressed as:

$$H^{(l+1)} = \sigma(\tilde{A}H^{(l)}W^{(l)}) \quad (9)$$

Where  $H^{(l)}$  is the node representation of layer  $l$ , and  $W^{(l)}$  is the learnable weight matrix of this layer. The formula shows that the representation of each node is obtained by the weighted combination of the features of its neighborhood nodes, and the feature is updated by linear transformation and nonlinear activation. Through the convolution operation of multi-layer graph, the model can gradually capture a wider range of spatial dependencies, so as to effectively identify the urban expansion structure and its boundary characteristics.

Because urban spatial structure exhibits different organizational characteristics at different scales, it is difficult to fully capture the urban development pattern using feature transmission at a single scale. Therefore, the model introduces the multi-scale spatial feature aggregation mechanism after the convolution of the map. Let the network contain the convolution structure of  $L$ -layer graph, then the node representations of different layers are  $H^{(1)}, H^{(2)}, \dots, H^{(L)}$  [24],[25]. In order to integrate spatial information of different scales, these representations are

weighted and combined, as follows:

$$H^* = \sum_{l=1}^L \alpha_l H^{(l)} \quad (10)$$

Where  $\alpha_l$  is a learnable scale weight parameter, which is used to control the contribution of different layer features in the final representation. This multi-scale aggregation method can make use of the local neighborhood structure and the far spatial dependence at the same time, so as to improve the expression ability of the model to the complexity of urban spatial structure.

After completing the spatial feature learning, it is necessary to map the node representation to the prediction results of the urban development boundary. Considering that the identification of urban development boundary can be regarded as a node classification problem in essence, the output layer of the model uses a linear classifier to predict. Let the final node be expressed as  $H^*$ , then the probability that each node belongs to the urban development area can be expressed as:

$$P_i = \text{Softmax}(H_i^* W_o + b_o) \quad (11)$$

Where  $H_i^*$  is the final eigenvector of node  $i$ ,  $W_o$  is the output layer weight matrix,  $b_o$  is the offset parameter, and softmax function is used to convert the output to probability distribution. According to the prediction probability, the node category label can be obtained, so as to identify the spatial units belonging to the development area or non-development area in urban space. Further combining with the spatial continuity rules, continuous urban development boundaries can be generated.

#### 4. IMPROVED GRAPH NEURAL NETWORK ALGORITHM FOR UGB DELINEATION

In the UGB delineation task, although traditional graph neural networks can capture topological dependencies between spatial units, they still face challenges in adequately representing spatial constraints and characterizing the driving mechanisms of urban expansion. To enhance the model's ability to represent urban spatial structure and development dynamics, this study proposes an improved graph neural network algorithm for UGB delineation. By introducing a spatial constraint mechanism, embedding urban expansion driving factors, learning adaptive neighborhood weights, and improving the graph attention structure, the model achieves high-precision urban development boundary identification and prediction.

Firstly, in order to enhance the ability of the model to describe the relationship between spatial planning constraints and geographical proximity, this study proposes a graph convolution calculation method for spatial constraint perception. In the process of urban development, the impact of different spatial units not only depends on the adjacency relationship, but also is affected by spatial constraints such as natural conditions, land policies and ecological protection red lines. Therefore, the spatial constraint weight matrix  $S$  is introduced into the graph convolution calculation to characterize the constraint relationship between spatial elements [26],[27]. Let the original adjacency matrix be  $A$  and the spatial constraint matrix be  $S$ , then the constraint enhanced adjacency matrix can be expressed as:

$$A^c = A \odot S \quad (12)$$

Where the symbol  $\odot$  represents element by element multiplication. The matrix  $S_{ij} \in [0,1]$  represents the spatial constraint strength between node  $i$  and node  $j$ . When some areas are restricted by ecological protection or development, the constraint weight is low, so as to reduce the impact of neighborhood propagation. On this basis, the convolution calculation process of spatial constraint graph can be expressed as:

$$H^{(l+1)} = \sigma \left( \widehat{D}^{-\frac{1}{2}} \widehat{A}^c \widehat{D}^{-\frac{1}{2}} H^{(l)} W^{(l)} \right) \quad (13)$$

Where  $\widehat{A}^c = A^c + I$  represents the adjacency matrix after adding self connection,  $\widehat{D}$  is the correspondence matrix,  $H^{(l)}$  is the representation of the node characteristics of the  $l$ st layer, and  $W^{(l)}$  is the learnable parameter matrix. The convolution mechanism of spatial constraint graph can reflect the constraints of spatial planning in the process of feature propagation, so as to improve the spatial rationality of UGB recognition.

Secondly, to enhance the model's ability to represent the dynamic mechanisms of urban expansion, this study introduces the embedding mechanism of urban expansion driving factors. Urban expansion is usually affected by traffic accessibility, economic development level, population density, land use structure and other factors, so these driving variables need to be integrated into the node feature representation [28],[29]. let the original node feature be  $h_i$  and the urban expansion driving factor vector be  $z_i$ , then the node representation after driving embedding can be expressed as:

$$\tilde{h}_i = h_i + W_d z_i \quad (14)$$

Where  $W_d$  is the driving factor mapping matrix, which is used to project the driving variables into the same representation space as the node characteristics. Through this embedding method, the dynamic information of urban development can be introduced into the learning process of graph structure, so that the spatial structure and development potential can be considered simultaneously in the boundary identification of the model.

In the process of neighborhood information dissemination, different neighborhood nodes have different influence on the target node. Therefore, this study proposes an adaptive neighborhood weight learning method to improve the propagation ability of spatial features by learning the dynamic weight relationship between nodes. Let the weight between node  $i$  and neighborhood node  $j$  be  $w_{ij}$ , then the weight is calculated by node feature similarity, and its expression is:

$$w_{ij} = \frac{\exp(\phi(h_i, h_j))}{\sum_{k \in N(i)} \exp(\phi(h_i, h_k))} \quad (15)$$

Where  $N(i)$  represents the neighborhood set of node  $i$ , and  $\phi(\cdot)$  represents the node feature similarity function. This study defines the function in the form of linear mapping:

$$\phi(h_i, h_j) = (Wh_i)^T (Wh_j) \quad (16)$$

Where  $W$  is the characteristic transformation matrix. Through this normalized weight calculation method, the contribution degree of different neighborhood nodes in information dissemination can be dynamically adjusted according to their feature similarity, so as to more accurately reflect the correlation strength between urban spatial units.

To further improve the model's capability in recognizing urban development boundaries, this study introduces the improved graph attention mechanism based on the adaptive weight mechanism. The mechanism highlights the influence of key spatial elements on boundary formation by learning the attention coefficient between nodes. Let the attention coefficient between node  $i$  and neighborhood node  $j$  be  $\alpha_{ij}$ , and its calculation form is:

$$\alpha_{ij} = \frac{\exp(\text{LeakyReLU}(a^T [Wh_i \parallel Wh_j]))}{\sum_{k \in N(i)} \exp(\text{LeakyReLU}(a^T [Wh_i \parallel Wh_k]))} \quad (17)$$

Where  $a$  is the attention vector that can be learned,  $\parallel$  is the vector concatenation operation, and leakyReLU is the activation function. Through this mechanism, the model can

automatically identify the neighborhood nodes that play an important role in the formation of the boundary, allowing the spatial change characteristics of the urban fringe to be more accurately represented. The node feature update process can be expressed as:

$$h'_i = \sigma \left( \sum_{j \in N(i)} \alpha_{ij} W h_j \right) \quad (18)$$

The calculation process realizes the neighborhood feature aggregation based on attention weight, so as to enhance the recognition ability of the model to the boundary structure.

After completing the spatial feature learning, the UGB prediction results need to be optimized to improve the continuity and stability of boundary recognition. To this end, this study constructs an objective function for the UGB delineation task. If the prediction result of the model is  $P_i$  and the real label is  $y_i$ , then the loss function of the basic classification can be expressed as cross entropy loss:

$$L_{ce} = - \sum_{i=1}^n y_i \log(P_i) \quad (19)$$

In order to enhance the spatial continuity of the prediction results, the spatial smooth regular term is also introduced, and its expression is:

$$L_{sp} = \sum_{(i,j) \in E} w_{ij} \| P_i - P_j \|^2 \quad (20)$$

Where  $w_{ij}$  represents the spatial weight between nodes, which is used to enforce consistency in prediction results between adjacent nodes, so as to avoid excessive discretization of boundary prediction. The final model optimization objective function can be expressed as:

$$L = L_{ce} + \lambda L_{sp} \quad (21)$$

Where  $\lambda$  is a trade-off parameter, which is used to control the balance between classification accuracy and spatial continuity.

## 5. IMPLEMENTATION OF INTELLIGENT DELINEATION ALGORITHM FOR URBAN DEVELOPMENT BOUNDARY

After completing the structural design and algorithm improvement of the graph neural network model, a complete implementation workflow for the UGB intelligent delineation algorithm is constructed, enabling the model to automatically generate continuous and meaningful development boundaries from urban spatial graph data. The overall algorithm takes the urban spatial graph  $G = (V, E, X)$  as input, where  $V$  represents the set of spatial unit nodes,  $E$  represents the set of spatial relationship edges between nodes, and  $X$  represents the node attribute matrix. UGB intelligent delineation algorithm firstly constructs the graph structure and encodes the features of the input data, then carries out spatial feature propagation and node representation learning through the improved graph neural network model, and finally outputs the probability that each spatial unit belongs to the development area, and on this basis, generates the continuous urban development boundary. Let the graph neural network model be a function  $F(\cdot)$ , then the overall prediction process can be expressed as:

$$P = F(G; \Theta) \quad (22)$$

Where  $P = [P_1, P_2, \dots, P_n]$  represents the prediction probability that all spatial units belong to the development area, and  $\Theta$  represents the model parameter set. According to the prediction probability, the classification results of spatial units can be obtained, thus forming

the spatial distribution of urban development areas and non-development areas.

In the model training stage, the parameters of graph neural network need to be optimized by supervised learning mechanism. Let the real label of each node in the training sample be  $y_i \in \{0,1\}$ , where 1 represents a developed area and 0 represents an undeveloped area, then the node prediction probability  $P_i$  is calculated by the model output layer. The model training realizes parameter updating by minimizing the loss function, and its basic form is cross entropy loss:

$$L_{cls} = -\frac{1}{n} \sum_{i=1}^n [y_i \log(P_i) + (1 - y_i) \log(1 - P_i)] \quad (23)$$

Where  $n$  is the number of training nodes. The gradient of the loss function to the model parameters is calculated by the back-propagation algorithm, and the parameters are updated using the gradient descent method. The update formula is:

$$\Theta^{t+1} = \Theta^t - \eta \frac{\partial L}{\partial \Theta} \quad (24)$$

Where  $\eta$  is the learning rate and  $t$  is the number of training iterations. After the model training, the trained parameters can be used to infer and predict the unmarked urban spatial units, so as to obtain the distribution of development potential within the urban space.

In the model training phase, the parameters of the graph neural network are optimized using a supervised learning mechanism.

$$L = L_{ce} + \lambda L_{sp} \quad (25)$$

This function not only ensures the classification accuracy, but also enhances the spatial continuity of the prediction results through the spatial smoothing regular term  $L_{sp}$ . Where  $\lambda$  is a trade-off parameter, which is used to control the balance between classification accuracy and spatial continuity. Through the joint optimization strategy, the prediction results can not only maintain high classification accuracy, but also conform to the overall structural characteristics of urban spatial development.

After obtaining the node prediction probability, it is necessary to further generate a continuous urban development boundary. Firstly, the node is divided into development area set  $U$  and non-development area set according to the prediction probability threshold  $\tau$ , which is defined as:

$$U = \{v_i \mid P_i \geq \tau\} \quad (26)$$

Where  $\tau$  is the probability threshold parameter. Then the continuous development area is identified by spatial clustering and regional connectivity analysis, and its external contour is extracted as the urban development boundary. Let the development area set be  $U$ , then the boundary node set can be expressed as:

$$B = \{v_i \in U \mid \exists v_j \notin U, (i, j) \in E\} \quad (27)$$

This set represents all development nodes adjacent to the non-development area. By sorting and connecting these boundary nodes in space, continuous UGB boundary curves can be generated. To improve the planning rationality of the boundary shape, the spatial smoothing method can also be used to optimize the boundary, for example, the moving average or curve fitting method can be used to smooth the boundary points, which is expressed as:

$$\tilde{b}_i = \frac{1}{k} \sum_{j=i-\frac{k}{2}}^{i+\frac{k}{2}} b_j \quad (28)$$

Where  $b_i$  is the coordinates of the original boundary point,  $\tilde{b}_i$  is the position of the smoothed boundary, and  $k$  is the size of the smoothed window. This processing can reduce the irregular fluctuation of the boundary and make the generated results more in line with the actual urban planning needs.

In terms of algorithm performance, the complexity of the algorithm needs to be analyzed. Let the urban spatial graph contain  $n$  nodes and  $m$  edges, then the computational complexity of convolution operation of single-layer graph mainly comes from the multiplication of adjacency matrix and characteristic matrix, and its complexity can be expressed as  $O(mh)$ . Where  $h$  is the hidden feature dimension. When the model contains the convolution structure of  $L$ -level graph, the overall computational complexity is about  $O(Lmh)$ . Because the urban spatial map usually has a sparse structure, this complexity has good computational efficiency in practical applications. In addition, the graph neural network model can be accelerated by batch processing and graph sampling technology, such as using neighborhood sampling strategy to reduce the number of nodes per calculation, so as to further improve the scalability of the algorithm in large-scale urban spatial data.

## 6. EXPERIMENTAL DESIGN AND EVALUATION SYSTEM

To verify the effectiveness and stability of the proposed GNN-based UGB intelligent delineation algorithm, a systematic experimental design and evaluation system was constructed. A typical rapidly urbanizing area in eastern China was selected as the study area, characterized by significant urban expansion and complex land use structure, offering high research representativeness. The total area of the study area is approximately 1250 km<sup>2</sup>, including multiple urban functional areas and urban-rural transition zones. The data sources used in the experiment include a variety of spatial data and socio-economic data. Among them, remote sensing images are mainly from Landsat 8 OLI and Sentinel-2 MSI, with a spatial resolution of 10–30 m; land use data are from the national land resources monitoring database; and; Traffic network data is from OpenStreetMap (OSM); Population and economic data are from the statistical yearbook and urban planning database. In order to unify the spatial analysis scale, this study divides the study area into 500 m × 500 m regular grids, generates 5024 spatial unit nodes, and constructs the urban spatial map structure based on them.

In the data pre-processing stage, multi-source spatial data need to be processed uniformly to ensure the consistency of different data sources in spatial scale and attribute dimension. Firstly, the remote sensing image is atmospheric corrected, image mosaic and cutting, and the supervised classification method is used to extract the characteristics of building land, impervious surface ratio and vegetation index (NDVI). The calculation formula of NDVI is:

$$NDVI = \frac{NIR - RED}{NIR + RED} \quad (29)$$

$NIR$  represents near-infrared reflectance and  $RED$  represents red reflectance, which can effectively reflect the surface vegetation coverage [30],[31]. Then, the road density index is calculated for the traffic network data, and the calculation expression is:

$$D_{road} = \frac{L_{road}}{A} \quad (30)$$

Where  $L_{road}$  is the total length of the road in the space unit, and  $A$  is the unit area. The population density index is obtained by spatial interpolation of statistical population data, and

its calculation form is:

$$D_{pop} = \frac{P}{A} \quad (31)$$

Where  $P$  is the unit population. Through the above processing, the node attribute matrix containing multidimensional urban development characteristics can be constructed, and the training set, validation set and test set can be further divided. This study divides the data according to the proportion of 60%: 20%: 20%, including 3014 training nodes, 1005 verification nodes and 1005 test nodes.

In order to more intuitively explain the composition of the experimental data, [Table 1](#) shows the main data types used in the experiment and their basic attributes.

**Table 1. Experimental data sources and attribute information**

Data type	Data sources	Spatial resolution	Data usage
Remote sensing image	Landsat 8 / Sentinel-2	10–30 m	Extracting land cover and NDVI
Land use data	Land and resources database	30 m	Land use classification
Traffic network data	OpenStreetMap	Vector	Road density calculation
Demographic data	Statistical yearbook	Administrative district level	Population density estimation
Economic data	Urban statistical database	Administrative district level	Economic intensity index

In terms of experimental model design, in order to verify the performance advantages of the proposed method, a variety of typical deep learning and graph neural network models are selected as comparison methods, including traditional machine learning method random forest (RF), deep neural network MLP, classical graph convolution network GCN, graph attention network GAT and spatial convolution network GraphSAGE. All models were trained in the same data set and experimental environment to ensure the fairness of the experimental results. During the training, Adam optimizer is used, the learning rate is set to 0.001, the batch size is 64, and the maximum number of training rounds is 200. To avoid over fitting, dropout (0.5) and L2 regularization are used to constrain the model. The core experimental parameters of different models are shown in [Table 2](#).

**Table 2. Experimental parameter settings of each model**

Model	Number of layers	Hide dimensions	Learning rate	Dropout
MLP	3	128	0.001	0.5
GCN	2	128	0.001	0.5
GraphSAGE	2	128	0.001	0.5
GAT	2	128	0.001	0.5
Proposed	3	128	0.001	0.5

In order to systematically evaluate the accuracy and spatial rationality of UGB delineation results, this study constructed a multi index evaluation system, including classification accuracy, precision, recall, and F1 score is obtained by harmonic averaging to comprehensively [\[32\],\[33\]](#). The accuracy rate is used to measure the accuracy of the overall forecast, and its calculation

formula is:

$$Accuracy = \frac{TP + TN}{TP + TN + FP + FN} \quad (32)$$

$TP$  represents the number of nodes in the development area correctly identified,  $TN$  represents the number of nodes in the non-development area correctly identified,  $FP$  represents the number of nodes misjudged as the development area, and  $FN$  represents the number of nodes in the development area not identified. The accuracy rate and recall rate are used to evaluate the accuracy and completeness of the model in the identification of development areas, and their expressions are respectively:

$$Precision = \frac{TP}{TP + FP} \quad (33)$$

$$Recall = \frac{TP}{TP + FN} \quad (34)$$

On this basis, F1 score, obtained by harmonic averaging, is used to comprehensively measure model performance:

$$F1 = \frac{2 \times Precision \times Recall}{Precision + Recall} \quad (35)$$

In addition to the classification accuracy index, the spatial consistency index is also introduced to evaluate the continuity of UGB boundary. Let the set of adjacent node pairs be  $E$ , then the spatial consistency index can be expressed as:

$$SC = 1 - \frac{1}{|E|} \sum_{(i,j) \in E} |P_i - P_j| \quad (36)$$

Where  $P_i$  and  $P_j$  respectively represent the prediction probability of adjacent nodes. The higher the index, the more continuous the prediction results in space.

To further illustrate the distribution of experimental data, [Table 3](#) gives the statistical results of the nodes in the development area and non-development area in the training data.

**Table 3. Distribution of training data categories**

Category	Number of nodes	Proportion
Development Area	1720	57.1%
Undeveloped area	1294	42.9%
Total	3014	100%

Through the above experimental design, a complete UGB delineation experimental environment can be constructed. The selection of research area ensures that the experiment has realistic representativeness, multi-source data fusion enhances the ability of urban spatial feature expression, and multi model comparison experiment can systematically evaluate the performance advantages of the proposed algorithm. At the same time, the multi index evaluation system can not only measure the classification accuracy of the model, but also reflect the rationality of the UGB boundary in the spatial structure, providing a reliable evaluation basis for the analysis of subsequent experimental results.

## 7. EXPERIMENTAL RESULTS AND PERFORMANCE ANALYSIS

This section evaluates the performance of the proposed GNN-based UGB intelligent delineation algorithm through systematic experiments and compares it with various benchmark models. The experimental results are comprehensively evaluated in terms of UGB delineation accuracy, algorithm performance improvement, adaptability to different spatial scales, computational efficiency, and stability.

Firstly, the accuracy of UGB delineation of different models is compared and analyzed. The traditional machine learning model random forest (RF), deep neural network MLP and various graph neural network models (GCN, GraphSAGE, GAT) were selected as the comparison baseline. The performance results of each model on the test set are shown in [Table 4](#).

**Table 4. Comparison of UGB delineation accuracy across different models**

Model	Accuracy	Precision	Recall	AUC
Random Forest	0.841	0.832	0.809	0.872
MLP	0.853	0.846	0.821	0.884
GCN	0.878	0.871	0.854	0.903
GraphSAGE	0.884	0.879	0.861	0.910
GAT	0.891	0.885	0.872	0.916
Proposed	0.912	0.907	0.894	0.935

It can be seen from [Table 4](#) that the performance of traditional machine learning model in UGB recognition task is relatively low, while the performance of graph neural network model is significantly improved due to its ability to use spatial topology. The accuracy index of GCN and GraphSAGE reached 0.878 and 0.884 respectively, while the improved model proposed in this study boosts the accuracy to 0.912 by introducing spatial constraints and adaptive neighborhood mechanism, which was about 3.4% higher than the basic GCN model. In order to more intuitively show the performance differences of different models, [Figure 1](#) shows the comparison results of F1-score of each model.

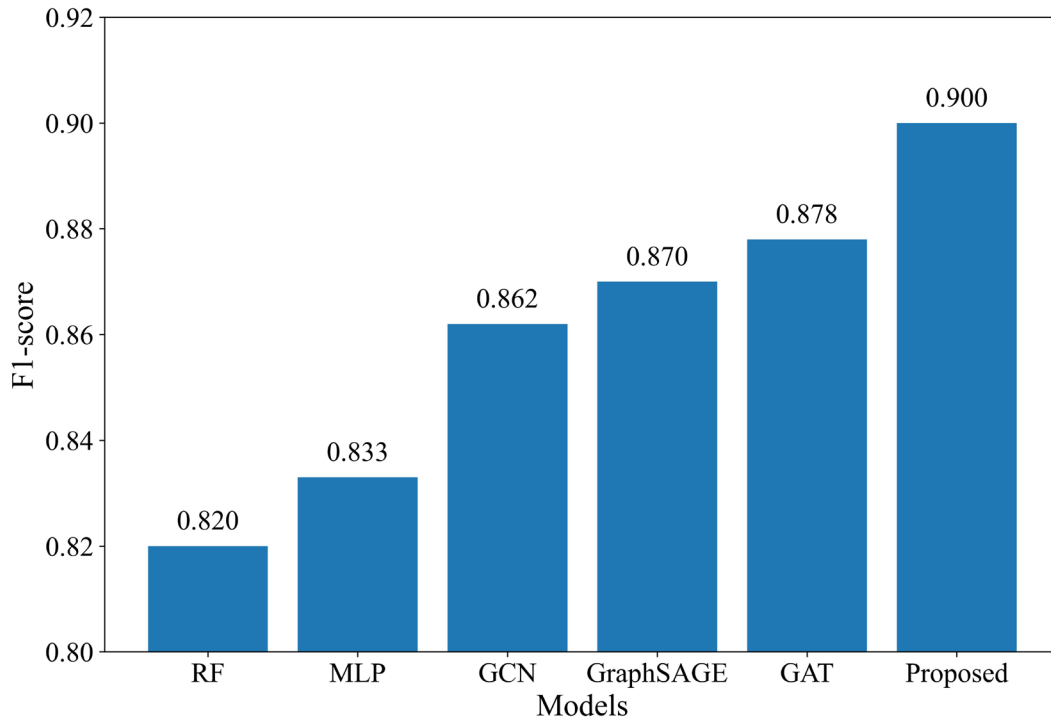


**Figure 1. Comparison of F1 scores across different models**

It can be seen from [Figure 1](#) that the graph neural network model is better than the traditional method as a whole, and the proposed method achieves the best results across all comprehensive metrics.

In order to further analyze the performance improvement effect brought by the algorithm improvement, the key modules of the model were gradually introduced into the experiment, including spatial constraint module (SC), driver embedding (DE) and adaptive neighborhood weight (AN). The experimental results are shown in [Table 5](#).

**Table 5. Contribution analysis of algorithmic modules**

Model structure	Accuracy	Precision	Recall	F1
Baseline GCN	0.878	0.871	0.854	0.862
GCN + SC	0.892	0.886	0.871	0.878
GCN + SC + DE	0.904	0.898	0.883	0.890
Complete model	0.912	0.907	0.894	0.900

As can be seen from [Table 5](#), the spatial constraint module improved accuracy by about 1.4%, and the embedding of driving factors further increased by 1.2%, while the adaptive neighborhood mechanism optimized the performance of the model. This shows that the driving factors of urban expansion and spatial constraint information play an important role in UGB recognition.

In order to evaluate the adaptability of the model at different spatial scales, experiments were conducted at four spatial grid scales: 250 m, 500 m, 750 m, and 1000 m. The model F1-score changes under different scales are shown in [Table 6](#).

**Table 6. Experimental results at different spatial scales**

Grid scale	RF	GCN	GAT	Proposed
250 m	0.811	0.856	0.871	0.889
500 m	0.820	0.862	0.878	0.900
750 m	0.813	0.854	0.870	0.892
1000 m	0.804	0.848	0.865	0.884

It can be found from [Table 6](#) that the model performance is the best when the grid scale is 500m. This is mainly because the scale can better balance the details of urban spatial structure and the overall regional characteristics.

In terms of spatial results, [Figure 2](#) shows the schematic diagram of UGB delineation results of the study area, in which the red area represents the predicted development area and the blue area represents the ecological or non-development area.

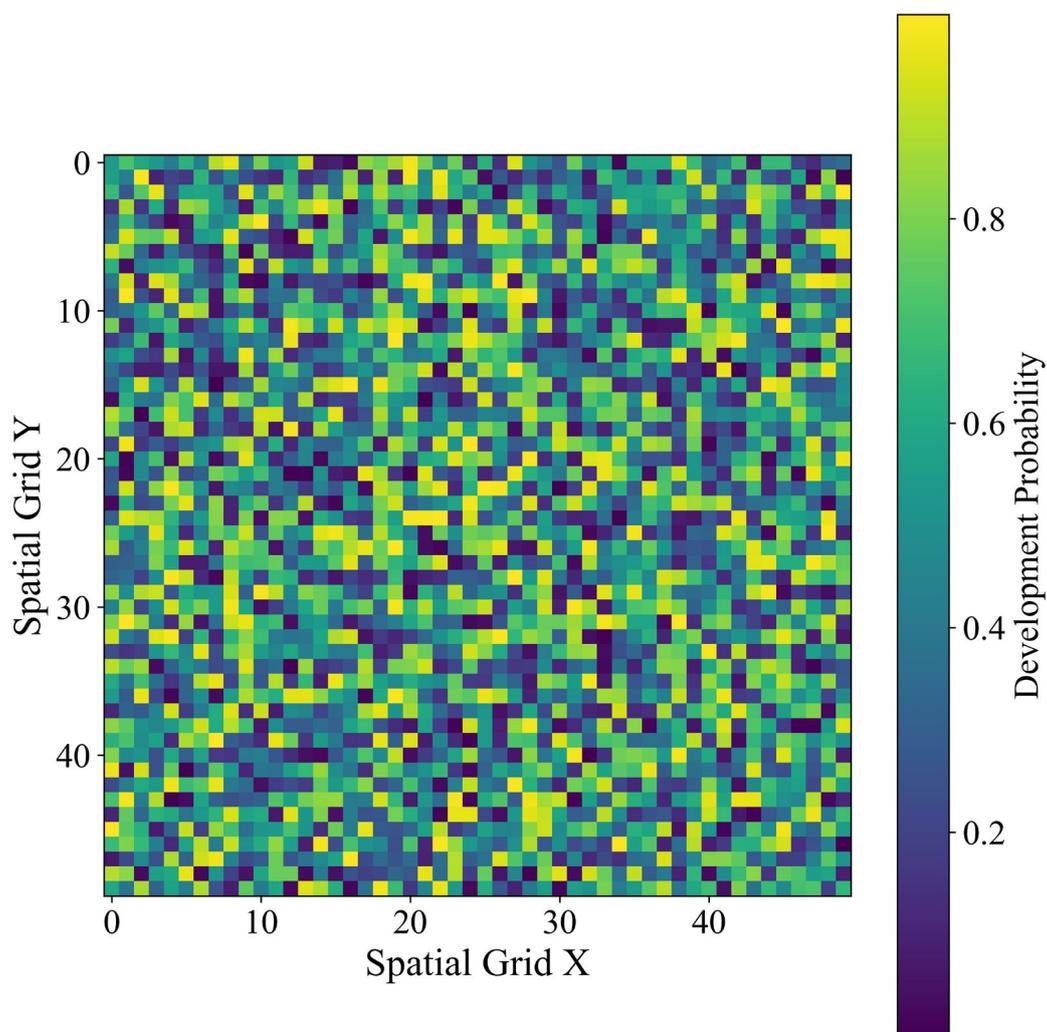


**Figure 2. Schematic diagram of the predicted urban development boundary**

It can be seen from [Figure 2](#) that the predicted UGB boundary is highly consistent with the actual urban expansion trend, and the boundary shape maintains good spatial continuity.

In terms of algorithm efficiency, the training time and reasoning time of each model are statistically analyzed. The calculation efficiency is defined as the calculation time per unit node, and its expression is:

$$T_{avg} = \frac{T_{total}}{n} \quad (37)$$

Where  $T_{total}$  is the total running time of the model, and  $n$  is the number of nodes. The experimental results are shown in [Table 7](#).

**Table 7. Comparison of model computational efficiency**

Model	Reasoning time (s)	Average node time (ms)
RF	4	0.79
MLP	6	1.04
GCN	8	1.26
GraphSAGE	9	1.35
GAT	11	1.50
Proposed	12	1.57

Although the computational cost of this method is slightly higher, it is within the acceptable range, and in exchange for a significant improvement in accuracy. [Figure 3](#) shows the comparison of training time of different models.

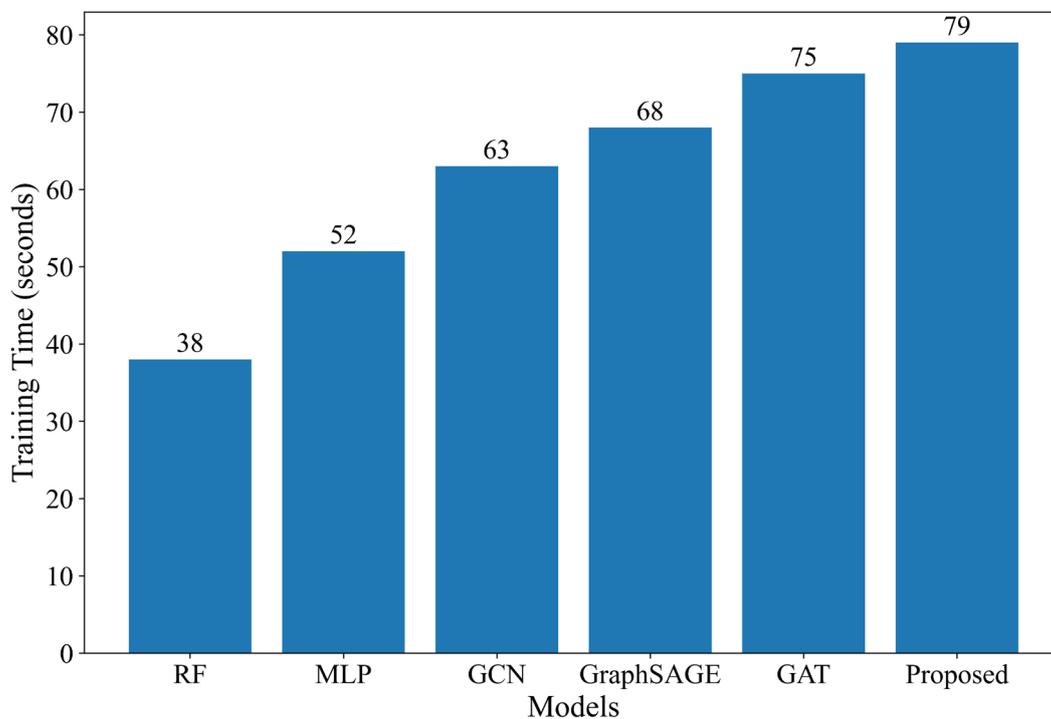


**Figure 3. Comparison of training time across different models**

In order to further verify the stability of the model, 10 repeated experiments were

conducted and the performance variance was calculated. The stability index is defined as:

$$\sigma = \sqrt{\frac{1}{k} \sum_{i=1}^k (F1_i - \bar{F1})^2} \quad (38)$$

Where  $k$  is the number of experiments. The experimental results are shown in [Table 8](#).

**Table 8. Model stability analysis**

Model	Average F1	Variance
RF	0.820	0.0042
MLP	0.833	0.0038
GCN	0.862	0.0027
GAT	0.878	0.0023
Proposed	0.900	0.0018

The results show that the proposed model is not only superior to other methods in accuracy, but also shows lower variance in many experiments, indicating that the algorithm has higher stability.

Based on the above experimental results, it can be concluded that the proposed UGB intelligent delineation algorithm based on graph neural network is superior to the traditional model in accuracy, stability and spatial adaptability. The model can effectively capture the urban spatial structure and expansion law, and still maintain good performance under different spatial scales. At the same time, the computational efficiency is within the acceptable range, which has strong practical application potential.

## 8. ABLATION EXPERIMENT AND MODEL MECHANISM ANALYSIS

To deeply analyze the contribution of key components in the proposed model to UGB identification performance, this section systematically verifies the core modules through ablation experiments and mechanism analysis. The experiments focus on the contribution of key modules, the effectiveness of the spatial constraint mechanism, the effect of the improved graph attention structure, and parameter sensitivity and robustness. All experiments were conducted under the same training data and experimental environment, with F1-score, accuracy, and AUC used as the main evaluation metrics. In order to measure the stability of the model prediction results, the model stability index is defined as:

$$Stability = 1 - \frac{1}{k} \sum_{i=1}^k |F1_i - \bar{F1}| \quad (39)$$

Where  $F1_i$  is the F1-score obtained in the  $i$ th experiment,  $\bar{F1}$  is the average F1-score, and  $k$  is the number of experimental repetitions. The closer the index is to 1, the more stable the model is under different experimental conditions.

Firstly, the contribution of key modules of the model to the overall performance is analyzed. This model mainly includes three core modules: spatial constraint graph convolution module (SC-GCN), urban expansion driver embedding module (DE), and adaptive graph attention module (AGA). By gradually removing each module to build a model with different structure

for comparative experiments. [Table 9](#) shows the performance changes of the model under different module combinations.

**Table 9. Contribution analysis of key model modules**

Model structure	Accuracy	Precision	Recall	F1-score	AUC
Basis GCN	0.878	0.871	0.854	0.862	0.903
GCN + SC	0.892	0.886	0.871	0.878	0.915
GCN + DE	0.895	0.889	0.874	0.881	0.918
GCN + AGA	0.901	0.895	0.883	0.889	0.924
GCN + SC + DE	0.904	0.898	0.883	0.890	0.929
Complete model	0.912	0.907	0.894	0.900	0.935

As can be seen from [Table 9](#), each module can significantly improve the performance of the model. The adaptive graph attention module contributes the most to the performance, and improves F1-score by about 2.7%. When the three modules work at the same time, the overall performance of the model reaches the best state.

In order to verify the effectiveness of spatial constraint mechanism in UGB delineation, the spatial consistency index (SC) is introduced for evaluation, and its calculation formula is:

$$SC = 1 - \frac{1}{|E|} \sum_{(i,j) \in E} |P_i - P_j| \quad (40)$$

Where  $P_i$  and  $P_j$  are the prediction probabilities of adjacent nodes respectively, and  $|E|$  is the number of edges in the graph. The higher the index, the more continuous the spatial prediction results. The experimental results are shown in [Table 10](#).

**Table 10. Validation of the spatial constraint mechanism**

Model	Accuracy	F1	Spatial Consistency
GCN	0.878	0.862	0.814
GCN + SC	0.892	0.878	0.847
GAT	0.891	0.878	0.838
Proposed	0.912	0.900	0.873

It can be seen from [Table 10](#) that after the introduction of spatial constraint mechanism, the spatial consistency index increased from 0.814 to 0.873, indicating that the prediction boundary is more continuous in space. [Figure 4](#) shows the change of UGB boundary before and after spatial constraints.

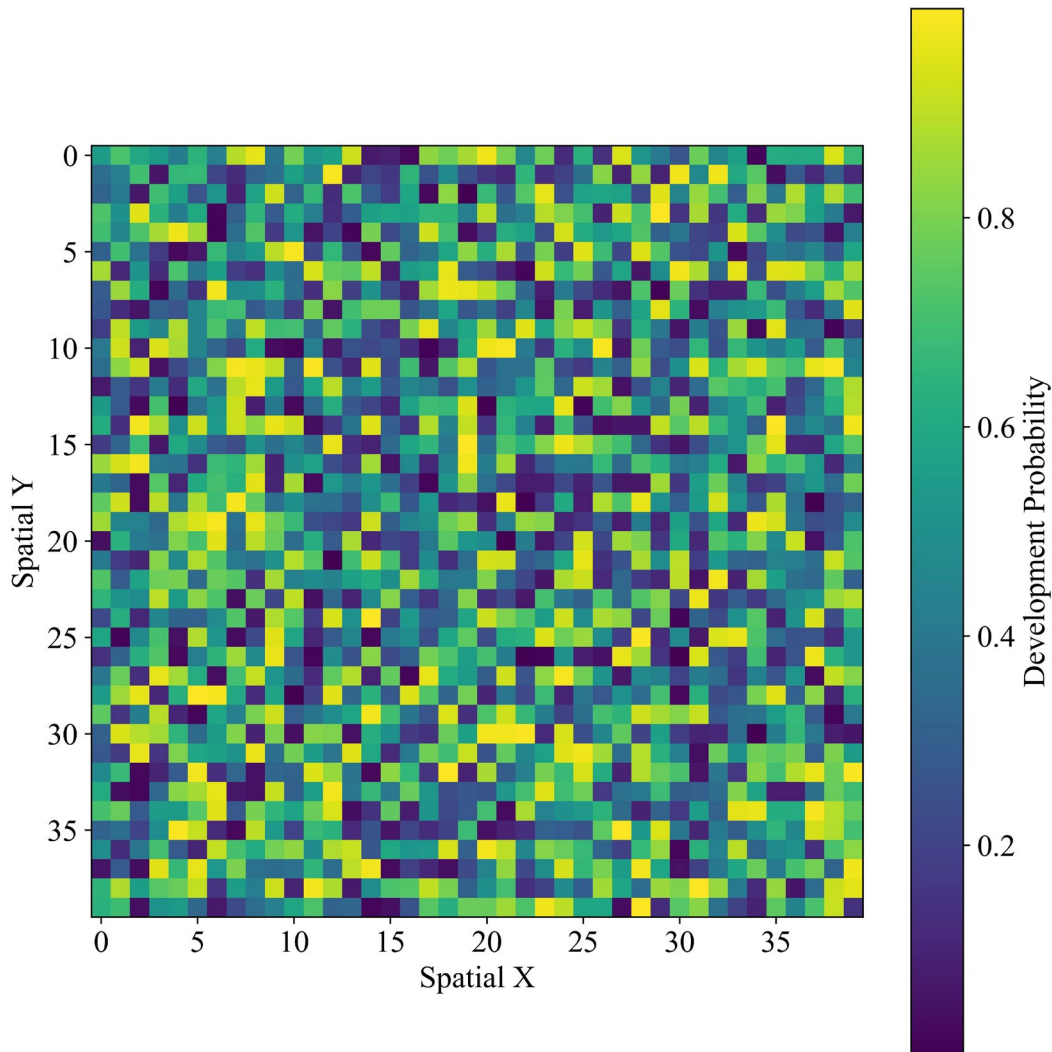


**Figure 4. UGB boundary before and after applying spatial constraints**

It can be observed that the prediction boundary is smoother and more continuous after adding spatial constraints.

In the aspect of graph attention mechanism, this study improves the traditional gat structure. This study adjusts attention by introducing the spatial distance weight  $d_{ij}$ :

$$\alpha_{ij}^* = \frac{\exp(\text{LeakyReLU}(a^T [Wh_i \parallel Wh_j] - \beta d_{ij}))}{\sum_{k \in N(i)} \exp(\text{LeakyReLU}(a^T [Wh_i \parallel Wh_k] - \beta d_{ik}))} \quad (41)$$

Where  $\beta$  is the distance attenuation parameter. This mechanism can enhance the influence of adjacent nodes and suppress the interference of long-distance nodes.

Further statistical analysis is made on the distribution of attention weight, and the results are shown in [Table 11](#).

**Table 11. Statistics of attention weight distribution**

Node distance interval	Traditional GAT weights	Improved GAT weights
------------------------	-------------------------	----------------------

0–500 m	0.21	0.34
500–1000 m	0.19	0.26
1000–1500 m	0.17	0.19
1500–2000 m	0.16	0.12
>2000 m	0.27	0.09

The results show that the improved attention mechanism significantly refines the weight distribution for adjacent nodes, making the model more consistent with the principles of urban spatial interaction.

In the aspect of parameter sensitivity analysis, the effects of hidden layer dimension  $h$ , learning rate  $\eta$  and spatial constraint weight  $\lambda$  on the performance of the model are investigated. The experimental setup  $h \in \{64,128,256,512\}$ , and the results are shown in [Table 12](#).

**Table 12. Sensitivity analysis of hidden layer dimensions**

Hidden size	Accuracy	F1
64	0.891	0.878
128	0.912	0.900
256	0.908	0.897
512	0.904	0.893

In addition, the sensitivity experiment of the spatial constraint parameter  $\lambda$  is also carried out, and the experimental results are shown in [Table 13](#).

**Table 13. Sensitivity analysis of spatial constraint parameters**

$\lambda$	Accuracy	F1
0	0.892	0.878
0.2	0.904	0.889
0.4	0.912	0.900
0.6	0.909	0.897
0.8	0.903	0.892

Finally, the robustness of the model is evaluated by repeated experiments. The experiment conducted 10 times of random initialization training, and the statistical results are shown in [Table 14](#).

**Table 14. Model robustness analysis**

Model	Average F1	Standard deviation
-------	------------	--------------------

RF	0.820	0.0042
MLP	0.833	0.0038
GCN	0.862	0.0027
GAT	0.878	0.0023
Proposed	0.900	0.0018

The experimental results show that the proposed model is not only superior to the benchmark method in accuracy, but also shows lower performance fluctuation in many experiments, indicating that the model has strong robustness and stability.

To sum up, through systematic ablation experiments and mechanism analysis, it can be found that spatial constraint mechanism, driver embedding and improved map attention structure can significantly improve the performance of UGB delineation. At the same time, the model has good stability for parameter changes, and can still maintain high prediction accuracy under different experimental conditions. These experimental results further verify the effectiveness and reliability of the proposed method in the task of intelligent delineation of urban development boundary.

## 9. CONCLUSIONS AND FUTURE RESEARCH DIRECTIONS

Focusing on the intelligent delineation of UGB, this study proposes a spatial structure learning method based on graph neural networks and constructs an automatic UGB recognition framework tailored for urban spatial planning. By abstracting urban spatial units as graph nodes and using multi-source spatial data to construct node attributes, the structural representation of the urban spatial system is realized. An improved graph neural network integrating spatial constraint information and urban expansion driving factors is designed. Through spatial feature encoding, graph convolution information propagation, and multi-scale feature aggregation, deep learning of urban spatial structure relationships is achieved. The experimental results show that the proposed method is superior to the traditional machine learning method and the classical graph neural network model in UGB recognition accuracy, spatial consistency and model stability, and can more accurately identify the urban development boundary and spatial expansion trends. At the same time, the model can still maintain good prediction ability under different spatial scales, which shows that the method has strong adaptability in complex urban spatial system.

From the perspective of methodology, this study provides a new theoretical thinking for the delineation of urban development boundary. Traditional UGB delineation methods often rely on empirical rules or a single spatial evaluation model, making it difficult to effectively describe the complex structural relationships within an urban spatial system. In this study, the urban space problem is transformed into the graph structure learning problem, and the graph neural network is used to jointly model the neighborhood relationship and development momentum between spatial units, allowing urban spatial topological relationships to be fully leveraged within a deep learning framework. In addition, by introducing the spatial constraint mechanism and embedding the driving factors of urban expansion into the model, the model can not only consider the spatial adjacency relationship, but also comprehensively reflect the impact of traffic conditions, population distribution and economic development on urban expansion. This modeling method combining spatial structure and urban development dynamics provides a new technical path for urban spatial planning research, and also opens up new research directions for the application of graph neural networks in the field of geospatial analysis.

At the practical application level, the UGB intelligent delineation method based on graph neural network has high application potential. With the development of remote sensing technology and geographic information system, the ability to obtain urban spatial data has been continuously improved. Large scale multi-source spatial data has become an important basic data for land spatial planning. The model proposed in this study can automatically learn the rules of urban spatial structure in the multi-source data environment, and generate the development boundary results with spatial continuity, which can serve as a scientific reference for decision-making by urban planning departments. In the fields of urban master planning, land spatial planning and urban expansion management, this method can help planners identify potential development areas and ecological protection areas, so as to achieve a more reasonable land use structure. At the same time, this method can also update the urban development trend by updating the input data, making the UGB delineation process more dynamic and data-driven, and enhancing the intelligence of urban governance.

Although this method has achieved some research results in the intelligent delineation of urban development boundary, there remains room for further expansion and optimization. Future research can be carried out in many directions. First of all, urban development has obvious characteristics of time evolution, and the research presented in this study is primarily based on static spatial data modeling. Therefore, time series data can be further introduced to build a spatio-temporal map neural network model to realize the dynamic analysis of urban expansion process. By integrating multi period remote sensing images and socio-economic data, the urban growth trend can be predicted, so as to achieve dynamic UGB delineation. Secondly, we can combine the urban development scenario simulation method to explore the change rules of UGB under different policy and planning scenarios, and provide a more comprehensive analytical tool for urban planning decision-making. In addition, in the aspect of model structure, multi-layer graph structure or heterogeneous graph neural network can be further introduced to enhance the expression ability of the model for complex spatial relationships. Finally, with the continuous accumulation of large-scale urban data, how to improve the interpretability of the model while ensuring computational efficiency is also an important direction for future research.

In general, the intelligent delineation method of urban development boundary based on graph neural network proposed in this study provides a new technical framework for intelligent analysis of complex urban spatial systems. This method can not only effectively integrate multi-source spatial data, but also capture the key patterns of urban spatial development through graph structure learning, providing data-driven decision support for urban planning and land spatial management. In the future, with the continuous development of deep learning technology and spatial data analysis methods, spatial planning research based on graph neural network is expected to play a more important role in urban governance, land use optimization and sustainable urban development.

## Abbreviations

GNN, Graph Neural Network;  
UGB, Urban Growth Boundary;  
GCN, Graph Convolutional Network;  
GAT, Graph Attention Network;  
MLP, Multilayer Perceptron;  
RF, Random Forest;  
NDVI, Normalized Difference Vegetation Index;  
OSM, OpenStreetMap;  
SC, Spatial Constraint;  
DE, Driver Embedding;  
AGA, Adaptive Graph Attention;  
AUC, Area Under the Curve;  
ReLU, Rectified Linear Unit;

### **Supplementary Material**

Not applicable.

### **Appendix**

Not applicable.

### **Ethics approval and consent to participate.**

This study did not involve human participants, animal subjects, or any data requiring ethical approval. Therefore, ethics approval and consent to participate are not applicable.

### **Acknowledgements**

The authors would like to thank the editors of this journal and all the anonymous reviewers who provided valuable comments on this work.

### **Competing interests**

The authors declare that they have no financial or personal relationships that may have inappropriately influenced them in writing this article.

### **Author contributions**

All authors have read and agreed to the published version of the manuscript. The author's contributions are specified as follows: **Y.L.:** Conceptualization, Methodology, Software, Validation, Formal analysis, Investigation, Data Curation, Writing – Original draft, Writing – Review & Editing, Visualization, Supervision, Project administration. **X.M.:** Conceptualization, Methodology, Software, Validation, Formal analysis, Investigation, Data Curation, Writing – Original draft, Writing – Review & Editing, Visualization, Supervision, Project administration.

### **Funding information**

The authors declare that no funds, grants, or other support were received during the preparation of this manuscript.

### **Data availability**

The data that support the findings of this study are available upon request from the corresponding authors, **Y.L.**

### **Disclaimer**

The views and opinions expressed in this article are those of the authors and are the product

of professional research. It does not necessarily reflect the official policy or position of any affiliated institution, funder, agency, or that of the publisher. The authors are responsible for this article's results, findings, and content.

### Declaration of AI and AI-assisted Technologies in the Writing Process

During the writing of this article, the author used ChatGPT 5 for spelling and grammar checking. After using this tool, the author reviewed and edited the content as needed and assumes full responsibility for the final published content.

### REFERENCES

- [1] Ma, S., Zhao, Y., & Tan, X. (2020). Exploring smart growth boundaries of urban agglomeration with land use spatial optimization: A case study of Changsha-Zhuzhou-Xiangtan city group, China. *Chinese Geographical Science*, 30(4), 665-676. DOI: <https://doi.org/10.1007/s11769-020-1140-1>
- [2] Liu, X., Shi, W., & Zhang, S. (2022). Progress of research on urban growth boundary and its implications in Chinese studies based on bibliometric analysis. *International Journal of Environmental Research and Public Health*, 19(24), 16644. DOI: <https://doi.org/10.5604/01.3001.0055.2685>
- [3] Wei, J., Yue, W., Li, M., Liu, Y., & Song, Y. (2025). Multi-scenario urban growth boundaries and trade-offs among land use functions. *Cities*, 159, 105752. DOI: <https://doi.org/10.1016/j.cities.2025.105752>
- [4] Li, Z., Luan, W., Zhang, Z., & Su, M. (2020). Relationship between urban construction land expansion and population/economic growth in Liaoning Province, China. *Land Use Policy*, 99, 105022. DOI: <https://doi.org/10.1016/j.landusepol.2020.105022>
- [5] Colsaet, A., Laurans, Y., & Levrel, H. (2018). What drives land take and urban land expansion? A systematic review. *Land Use Policy*, 79, 339-349. DOI: <https://doi.org/10.1016/j.landusepol.2018.08.017>
- [6] Mahtta, R., Fragkias, M., Güneralp, B., Mahendra, A., Reba, M., Wentz, E. A., & Seto, K. C. (2022). Urban land expansion: the role of population and economic growth for 300+ cities. *Npj Urban Sustainability*, 2(1), 5. DOI: <https://doi.org/10.1038/s42949-022-00048-y>
- [7] Zhang, T., Wu, K., Wang, X., Li, X., Li, L., & Chen, L. (2025). Impact of land use patterns on flood risk in the Chang-Zhu-Tan urban agglomeration, China. *Remote Sensing*, 17(16), 2889. DOI: <https://doi.org/10.3390/rs17162889>
- [8] Wang, Z., & Ren, F. (2025). Developing a decision support system for sustainable urban planning using machine learning-based scenario modeling. *Scientific Reports*, 15(1), 13210. DOI: <https://doi.org/10.1038/s41598-025-90057-5>
- [9] Wagner, M., & de Vries, W. T. (2019). Comparative review of methods supporting decision-making in urban development and land management. *Land*, 8(8), 123. DOI: <https://doi.org/10.3390/land8080123>
- [10] Wu, Z., Pan, S., Chen, F., Long, G., Zhang, C., & Yu, P. S. (2020). A comprehensive survey on graph neural networks. *IEEE transactions on neural networks and learning systems*, 32(1), 4-24. DOI: <https://doi.org/10.55041/IJSREM55073>
- [11] Khemani, B., Patil, S., Kotecha, K., & Tanwar, S. (2024). A review of graph neural networks: concepts, architectures, techniques, challenges, datasets, applications, and

future directions. *Journal of Big Data*, 11(1), 18. DOI: [https://doi.org/10.1007/978-3-032-04315-3\\_1](https://doi.org/10.1007/978-3-032-04315-3_1)

- [12] Chen, Y., Zhao, P., Lin, Y., Sun, Y., Chen, R., Yu, L., & Liu, Y. (2024). Semantic-enhanced graph convolutional neural networks for multi-scale urban functional-feature identification based on human mobility. *ISPRS International Journal of Geo-Information*, 13(1), 27. DOI: <https://doi.org/10.3390/ijgi13010027>
- [13] Liu, Y., Guo, Q., & Zheng, C. (2025). Urban street network morphology classification through street-block based graph neural networks and multi-model fusion. *International Journal of Digital Earth*, 18(1), 2497490. DOI: <https://doi.org/10.1080/17538947.2025.2497490>
- [14] Wu, P., Zhang, Z., Peng, X., & Wang, R. (2024). Deep learning solutions for smart city challenges in urban development. *Scientific Reports*, 14(1), 5176. DOI: <https://doi.org/10.1038/s41598-024-55928-3>
- [15] Wang, S., Zhao, C., Jiang, Q., Zhu, D., Ma, J., & Sun, Y. (2025). Application of Graph Convolutional Neural Networks and multi-sources data on urban functional zones identification, A case study of Changchun, China. *Sustainable Cities and Society*, 119, 106116. DOI: <https://doi.org/10.1016/j.scs.2024.106116>
- [16] Cai, C., Guo, Z., Zhang, B., Wang, X., Li, B., & Tang, P. (2021). Urban morphological feature extraction and multi-dimensional similarity analysis based on deep learning approaches. *Sustainability*, 13(12), 6859. DOI: <https://doi.org/10.3390/su13126859>
- [17] Liang, Y., Zhu, J., Ye, W., & Gao, S. (2022, November). Region2Vec: community detection on spatial networks using graph embedding with node attributes and spatial interactions. In *Proceedings of the 30th international conference on advances in geographic information systems* (pp. 1-4). DOI: <https://doi.org/10.1145/3557915.3560974>
- [18] Xie, X., Mao, W., Yang, Z., Hu, S., Xu, Y., Wu, L., & Xie, Z. (2025). A hybrid spatial learning method integrating graph neural networks and explainable AI to understand urban vitality. *Sustainable Cities and Society*, 106920. DOI: <https://doi.org/10.1016/j.scs.2025.106920>
- [19] Chen, D., Feng, Y., Li, X., Qu, M., Luo, P., & Meng, L. (2025). Interpreting core forms of urban morphology linked to urban functions with explainable graph neural network. *Computers, Environment and Urban Systems*, 118, 102267. DOI: <https://doi.org/10.1016/j.compenvurbsys.2025.102267>
- [20] Ding, C., Tang, J., Zhang, M., Wu, H., & Wang, B. (2026). Identifying dynamic functions of urban areas with a multi-temporal collaborative graph neural network model. *International Journal of Geographical Information Science*, 40(1), 78-111. DOI: <https://doi.org/10.1080/13658816.2025.2517195>
- [21] Corso, G., Cavalleri, L., Beaini, D., Liò, P., & Veličković, P. (2020). Principal neighbourhood aggregation for graph nets. *Advances in neural information processing systems*, 33, 13260-13271. DOI: <https://dl.acm.org/doi/10.5555/3495724.3496836>
- [22] Dong, W., Wu, J., Luo, Y., Ge, Z., & Wang, P. (2022). Node representation learning in graph via node-to-neighbourhood mutual information maximization. In *Proceedings of the IEEE/CVF Conference on Computer Vision and Pattern Recognition* (pp. 16620-16629). DOI: <https://doi.org/10.1109/CVPR52688.2022.01612>
- [23] Wang, P., Han, J., Li, C., & Pan, R. (2019, July). Logic attention based neighborhood aggregation for inductive knowledge graph embedding. In *Proceedings of the AAAI conference on artificial intelligence* (Vol. 33, No. 01, pp. 7152-7159). DOI: <https://doi.org/10.1609/aaai.v33i01.33017152>

- [24] You, Y., Chen, T., Wang, Z., & Shen, Y. (2020). L2-gcn: Layer-wise and learned efficient training of graph convolutional networks. In *Proceedings of the IEEE/CVF conference on computer vision and pattern recognition* (pp. 2127-2135). DOI: <https://doi.org/10.1109/CVPR42600.2020.00220>
- [25] Miao, X., Zhang, W., Shao, Y., Cui, B., Chen, L., Zhang, C., & Jiang, J. (2021). Lasagne: A multi-layer graph convolutional network framework via node-aware deep architecture. *IEEE Transactions on Knowledge and Data Engineering*, 35(2), 1721-1733. DOI: <https://doi.org/10.1109/TKDE.2021.3103984>
- [26] Zhang, S., Tong, H., Xu, J., & Maciejewski, R. (2019). Graph convolutional networks: a comprehensive review. *Computational Social Networks*, 6(1), 1-23. DOI: <https://doi.org/10.1186/s40649-019-0069-y>
- [27] Diao, Z., Wang, X., Zhang, D., Liu, Y., Xie, K., & He, S. (2019, July). Dynamic spatial-temporal graph convolutional neural networks for traffic forecasting. In *Proceedings of the AAAI conference on artificial intelligence* (Vol. 33, No. 01, pp. 890-897). DOI: <https://doi.org/10.1609/aaai.v33i01.3301890>
- [28] Shi, G., Shan, J., Ding, L., Ye, P., Li, Y., & Jiang, N. (2019). Urban road network expansion and its driving variables: a case study of Nanjing City. *International journal of environmental research and public health*, 16(13), 2318. DOI: <https://doi.org/10.3390/ijerph16132318>
- [29] Karimi, F., & Sultana, S. (2024). Urban expansion prediction and land use/land cover change modeling for sustainable urban development. *Sustainability*, 16(6), 2285. DOI: <https://doi.org/10.3390/su16062285>
- [30] Zhao, W., Wu, J., Shen, Q., Liu, L., Lin, J., & Yang, J. (2022). Estimation of the net primary productivity of winter wheat based on the near-infrared radiance of vegetation. *Science of the Total Environment*, 838, 156090. DOI: <https://doi.org/10.1016/j.scitotenv.2022.156090>
- [31] Tian, Q., Jin, H., Fensholt, R., Tagesson, T., Feng, L., & Tian, F. (2026). Varying sensitivities of RED-NIR-based vegetation indices to the input reflectance affect the detected long-term trends. *ISPRS Journal of Photogrammetry and Remote Sensing*, 233, 247-265. DOI: <https://doi.org/10.1016/j.isprsjprs.2026.01.028>
- [32] Açıkkar, M., & Tokgöz, S. (2025). Improving multi-class classification: scaled extensions of harmonic mean-based adaptive k-nearest neighbors: M. Açıkkar and S. Tokgöz. *Applied Intelligence*, 55(3), 168. DOI: <https://doi.org/10.1007/s10489-024-06109-2>
- [33] Seredin, O. S., & Kopylov, A. V. (2024). Harmonic Averaging in Classifier Quality Assessment. *Pattern Recognition and Image Analysis*, 34(4), 1160-1171. DOI: <https://doi.org/10.1134/S1054661824701220>